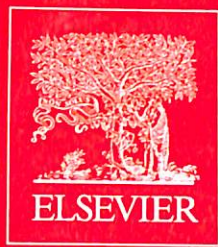


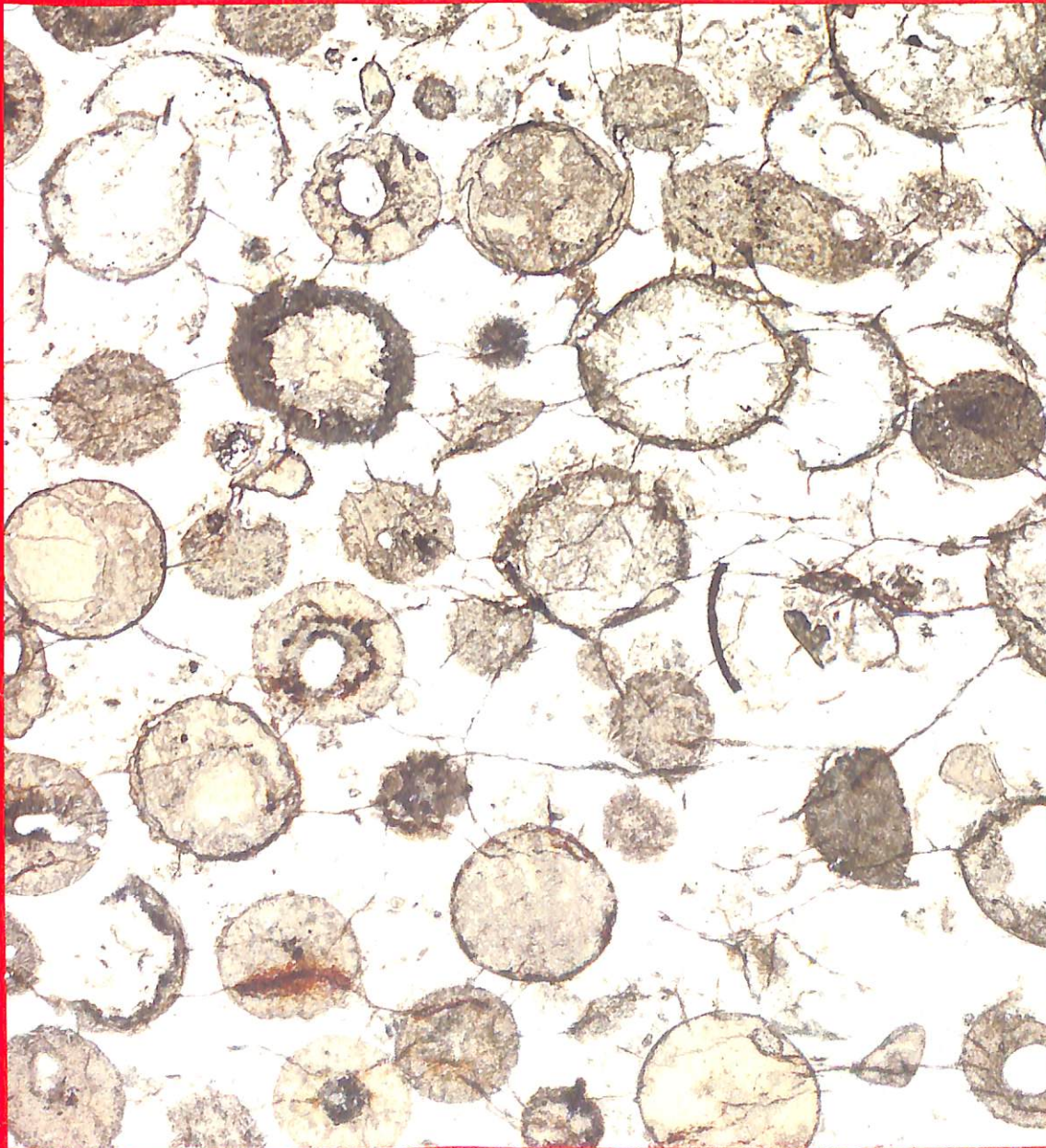
Volume 224

January 2013

ISSN 0301-9268



PRECAMBRIAN RESEARCH



(Abstracts/contents lists published in Am. Geol. Inst. Bibliogr.; Abstr. Bull. Signalétique; Chem. Abstr.; Curr. Contents; Phys. Chem. Earth Sci., Geo Abstr.; Mineral Abstr.)

Pumice from the ~3460 Ma Apex Basalt, Western Australia: A natural laboratory for the early biosphere M.D. Brasier, R. Matthewman, S. McMahon, M.R. Kilburn and D. Wacey	1
Trading partners: Tectonic ancestry of southern Africa and western Australia, in Archean supercratons Vaalbara and Zimgarn A.V. Smirnov, D.A.D. Evans, R.E. Ernst, U. Söderlund and Z.-X. Li	11
Hydrothermal activity during Ediacaran-Cambrian transition: Silicon isotopic evidence H. Fan, H. Wen, X. Zhu, R. Hu and S. Tian	23
Geochemical and Hf-Nd isotopic constraints on the crustal evolution of Archean rocks from the Minnesota River Valley, USA A.M. Satkoski, M.E. Bickford, S.D. Samson, R.L. Bauer, P.A. Mueller and G.D. Kamenov	36
The La Tinta pole revisited: Paleomagnetism of the Neoproterozoic Sierras Bayas Group (Argentina) and its implications for Gondwana and Rodinia A.E. Rapalini, R.I. Trindade and D.G. Poiré	51
Episodic Paleoproterozoic (~2.45, ~1.95 and ~1.85 Ga) mafic magmatism and associated high temperature metamorphism in the Daqingshan area, North China Craton: SHRIMP zircon U-Pb dating and whole-rock geochemistry Y. Wan, Z. Xu, C. Dong, A. Nutman, M. Ma, H. Xie, S. Liu, D. Liu, H. Wang and H. Cu	71
Geochemistry of ~2.7 Ga basalts from Taishan area: Constraints on the evolution of early Neoproterozoic granite-greenstone belt in western Shandong Province, China W. Wang, E. Yang, M. Zhai, S. Wang, M. Santosh, L. Du, H. Xie, B. Lv and Y. Wan	94
Geochemistry of a komatiitic, boninitic, and tholeiitic basalt association in the Mesoarchean Koolyanobbing greenstone belt, Southern Cross Domain, Yilgarn craton: Implications for mantle sources and geodynamic setting of banded iron formation T. Angerer, R. Kerrich and S.G. Hagemann	110
U-Pb age and Hf-isotope geochemistry of zircon from felsic volcanic rocks of the Paleoproterozoic Aillik Group, Makkovik Province, Labrador C. LaFlamme, P.J. Sylvester, A.M. Hinchey and W.J. Davis	129
Stabilization of the southern portion of the São Francisco craton, SE Brazil, through a long-lived period of potassic magmatism R. Romano, C. Lana, F.F. Alkmim, G. Stevens and R. Armstrong	143
Dating the termination of the Palaeoproterozoic Lomagundi-Jatuli carbon isotopic event in the North Transfennoscandian Greenstone Belt A.P. Martin, D.J. Condon, A.R. Prave, V.A. Melezhik, A. Lepland and A.E. Fallick	160
Isotopic composition of organic and inorganic carbon from the Mesoproterozoic Jixian Group, North China: Implications for biological and oceanic evolution H. Guo, Y. Du, L.C. Kah, J. Huang, C. Hu, H. Huang and W. Yu	169

(Contents continued on BM III)

CAPTION FOR COVER PHOTOGRAPH

3,243 million-year-old spherules in the Fig Tree Group, Barberton Greenstone Belt, South Africa, formed as a result of large meteorite impacts on the early Earth. The 35-cm-thick spherule bed (S3) is composed of nearly pure spherules produced during the condensation of an impact-produced rock vapor cloud. The estimated diameter of the bolide was 20–50 km. The spherules, 0.5–1.5 mm in diameter in the photo, include silica-(clear), phyllosilicate- (gray), and rutile/anatase-rich (black) varieties; massive and layered types; and a few originally hollow spherules. This is one of four spherule layers in the Barberton Belt, ranging from 3,470–3,243 Ma, that represent the oldest known impact deposits and provide direct evidence for a significant flux of large impactors as late as 3.2 Ga. Photograph: D.R. Lowe



(Contents continued from back cover)

Zircon U-Pb-Hf isotopes and whole-rock geochemistry of granitoid gneisses in the Jianping gneissic terrane, Western Liaoning Province: Constraints on the Neoproterozoic crustal evolution of the North China Craton W. Wang, S. Liu, M. Santosh, X. Bai, Q. Li, P. Yang and R. Guo	184
Proterozoic evolution of the Mojave crustal province as preserved in the Ivanpah Mountains, southeastern California B.A. Strickland, J.L. Wooden, C.G. Mattinson, T. Ushikubo, D.M. Miller and J.W. Valley	222
2.46 Ga kalsilite and nepheline syenites from the Awsard pluton, Reguibat Rise of the West African Craton, Morocco. Generation of extremely K-rich magmas at the Archean-Proterozoic transition F. Bea, P. Montero, F. Haissen and A. El Archi	242
Tube construction and life mode of the late Ediacaran tubular fossil <i>Gaojiashania cyclus</i> from the Gaojiashan Lagerstätte Y. Cai, H. Hua and X. Zhang	255
Geochronological constraints on the magmatic and tectonic development of the Pongola Supergroup (Central Region), South Africa S.B. Mukasa, A.H. Wilson and K.R. Young	268
The growth, reworking and metamorphism of early Precambrian crust in the Jiaobei terrane, the North China Craton: Constraints from U-Th-Pb and Lu-Hf isotopic systematics, and REE concentrations of zircon from Archean granitoid gneisses J. Liu, F. Liu, Z. Ding, C. Liu, H. Yang, P. Liu, F. Wang and E. Meng	287
New interpretations on palaeomagnetic data from the Nagssugtoqidian mobile belt in Greenland G.E.J. Beckmann	304
Tectonic history of the North American shield recorded in uranium deposits in the Beaverlodge area, northern Saskatchewan, Canada S. Dieng, K. Kyser and L. Godin	316
Geochemical constraints on the origin of post-depositional fluids in sedimentary carbonates of the Ediacaran system in South China Y.-Y. Zhao and Y.-F. Zheng	341
Chemical and Sr-Nd isotopic compositions and zircon U-Pb ages of the Birimian granitoids from NE Burkina Faso, West African Craton: Implications on the geodynamic setting and crustal evolution B. Tapsoba, C.-H. Lo, B.-M. Jahn, S.-L. Chung, U. Wenmenga and Y. Iizuka	364
Geochemistry of gabbros and granitoids (M- and I-types) from the Nubian Shield of Egypt: Roots of Neoproterozoic intra-oceanic island arc A.E. Maurice, B.R. Bakhit, F.F. Basta and A.A. Khiamy	397
Petrology of high-pressure granulite facies metapelites and metabasites from Tcholliré and Banyo regions: Geodynamic implication for the Central African Fold Belt (CAFB) of north-central Cameroon M.H. Bouyo, J. Penaye, P. Barbey, S.F. Toteu and P. Wandji	412
Chromium isotope fractionation during oxidative weathering—Implications from the study of a Paleoproterozoic (ca. 1.9 Ga) paleosol, Schreiber Beach, Ontario, Canada R. Frei and A. Polat	434
The metacarbonate rocks of Itatuba (Paraíba): A record of sedimentary recycling in a Paleoproterozoic collision zone of the Borborema province, NE Brazil E.J. dos Santos, J.A. Souza Neto, L.C.M. Carmona, R. Armstrong, L.C.M.L. Santos and L.U.D.S. Mendes	454
2.6-2.7 Ga crustal growth in Yangtze craton, South China K. Chen, S. Gao, Y. Wu, J. Guo, Z. Hu, Y. Liu, K. Zong, Z. Liang and X. Geng	472
The origin of coexisting carbonates in banded iron formations: A micro-mineralogical study of the 2.4 Ga Itabira Group, Brazil R. Morgan, B. Orberger, C.A. Rosière, R. Wirth, C.d.M. Carvalho and M.T. Bellver-Baca	491
Late Paleoproterozoic terrane accretion in northwestern Canada and the case for circum-Columbian orogenesis F. Furlanetto, D.J. Thorkelson, H. Daniel Gibson, D.D. Marshall, R.H. Rainbird, W.J. Davis, J.L. Crowley and J.D. Vervoort	512
Proliferation of MISS-forming microbial mats after the late Neoproterozoic glaciations: Evidence from the Kimberley region, NW Australia Z.-W. Lan and Z.-Q. Chen	529
Local $\delta^{34}\text{S}$ variability in ~580 Ma carbonates of northwestern Mexico and the Neoproterozoic marine sulfate reservoir S.J. Loyd, P.J. Marenco, J.W. Hagadorn, T.W. Lyons, A.J. Kaufman, F. Sour-Tovar and F.A. Corsetti	551
Back-arc and post-collisional volcanism in the Palaeoproterozoic Granites-Tanami Orogen, Australia B. Li, L. Bagas, L.A. Gallardo, N. Said, C. Diwu and T.C. McCuaig	570
New palaeomagnetic and rock magnetic results on Mesoproterozoic kimberlites from the Eastern Dharwar craton, southern India: Towards constraining India's position in Rodinia M. Venkateshwarlu and N.V. Chalapathi Rao	588

Geochronology and geochemistry of Neoproterozoic magmatism in the Erguna Massif, NE China: Petrogenesis and implications for the breakup of the Rodinia supercontinent J. Tang, W.-L. Xu, F. Wang, W. Wang, M.-J. Xu and Y.-H. Zhang	597
Petrogenesis of Archean PGM-bearing chromitites and associated ultramafic-mafic-anorthositic rocks from the Guelb el Azib layered complex (West African craton, Mauritania) J. Berger, H. Diot, K. Lo, D. Ohnenstetter, O. Féménias, M. Pivin, D. Demaiffe, A. Bernard and B. Charlier	612
Clockwise, low- <i>P</i> metamorphism of the Aus granulite terrain, southern Namibia, during the Mesoproterozoic Namaqua Orogeny J.F.A. Diener, R.W. White, K. Link, T.S. Dreyer and A. Moodley	629
Neoproterozoic to early Cambrian Franciscan-type mélanges in the Teplá-Barrandia unit, Bohemian Massif: Evidence of modern-style accretionary processes along the Cadomian active margin of Gondwana? J. Hajná J. Žák, V. Kachlík, W. Dörr and A. Gerdes	653
Structural and geochronological constraints on the evolution of the eastern margin of the Tanzania Craton in the Mpwapwa area, central Tanzania R.J. Thomas, N.M.W. Roberts, J. Jacobs, A.M. Bushi, M.S.A. Horstwood and A. Mruma	671
Trace fossil evidence for Ediacaran bilaterian animals with complex behaviors Z. Chen, C. Zhou, M. Meyer, K. Xiang, J.D. Schiffbauer, X. Yuan and S. Xiao	690



Contents

Special Issue

Biogeochemical changes across the Ediacaran–Cambrian transition in South China

Guest Editors:

Graham Shields-Zhou, Maoyan Zhu

Biogeochemical changes across the Ediacaran–Cambrian transition in South China G. Shields-Zhou and M. Zhu	1
Carbon isotope chemostratigraphy and sedimentary facies evolution of the Ediacaran Doushantuo Formation in western Hubei, South China M. Zhu, M. Lu, J. Zhang, F. Zhao, G. Li, Y. Aihua, X. Zhao and M. Zhao	7
The biostratigraphic succession of acanthomorphic acritarchs of the Ediacaran Doushantuo Formation in the Yangtze Gorges area, South China and its biostratigraphic correlation with Australia P. Liu, C. Yin, S. Chen, F. Tang and L. Gao	29
Early embryogenesis of potential bilaterian animals with polar lobe formation from the Ediacaran Weng'an Biota, South China Z. Yin, M. Zhu, P. Tafforeau, J. Chen, P. Liu and G. Li	44
Petrographic analysis of new specimens of the putative microfossil <i>Vernanimalcula guizhouena</i> (Doushantuo Formation, South China) V.A. Petryshyn, D.J. Bottjer, J.-Y. Chen and F. Gao	58
Re-Os geochronology of black shales from the Neoproterozoic Doushantuo Formation, Yangtze platform, South China B. Zhu, H. Becker, S.-Y. Jiang, D.-H. Pi, M. Fischer-Gödde and J.-H. Yang	67
Greigite from carbonate concretions of the Ediacaran Doushantuo Formation in South China and its environmental implications J. Dong, S. Zhang, G. Jiang, H. Li and R. Gao	77
The DOUNCE event at the top of the Ediacaran Doushantuo Formation, South China: Broad stratigraphic occurrence and non-diagenetic origin M. Lu, M. Zhu, J. Zhang, G. Shields-Zhou, G. Li, F. Zhao, X. Zhao and M. Zhao	86
Cerium anomaly variations in Ediacaran-earliest Cambrian carbonates from the Yangtze Gorges area, South China: Implications for oxygenation of coeval shallow seawater H.-F. Ling, X. Chen, D. Li, D. Wang, G.A. Shields-Zhou and M. Zhu	110
Carbon and strontium isotope evolution of seawater across the Ediacaran-Cambrian transition: Evidence from the Xiaotan section, NE Yunnan, South China D. Li, H.-F. Ling, G.A. Shields-Zhou, X. Chen, L. Cremonese, L. Och, M. Thirlwall and C.J. Manning	128
Marine biogeochemical cycling during the early Cambrian constrained by a nitrogen and organic carbon isotope study of the Xiaotan section, South China L. Cremonese, G. Shields-Zhou, U. Struck, H.-F. Ling, L. Och, X. Chen and D. Li	148
Redox changes in Early Cambrian black shales at Xiaotan section, Yunnan Province, South China L.M. Och, G.A. Shields-Zhou, S.W. Poulton, C. Manning, M.F. Thirlwall, D. Li, X. Chen, H. Ling, T. Osborn and L. Cremonese	166

Irreversible change of the oceanic carbon cycle in the earliest Cambrian: High-resolution organic and inorganic carbon chemostratigraphy in the Three Gorges area, South China T. Ishikawa, Y. Ueno, D. Shu, Y. Li, J. Han, J. Guo, N. Yoshida and T. Komiya	190
High resolution organic carbon isotope stratigraphy from a slope to basinal setting on the Yangtze Platform, South China: Implications for the Ediacaran-Cambrian transition Q. Guo, H. Strauss, M. Zhu, J. Zhang, X. Yang, M. Lu and F. Zhao	209
Trace and rare earth element geochemistry of black shale and kerogen in the early Cambrian Niutitang Formation in Guizhou province, South China: Constraints for redox environments and origin of metal enrichments D.-H. Pi, C.-Q. Liu, G.A. Shields-Zhou and S.-Y. Jiang	218

(Abstracts/contents lists published in *Am. Geol. Inst. Bibliogr.*; *Abstr. Bull. Signalétique*; *Chem. Abstr.*; *Curr. Contents*; *Phys. Chem. Earth Sci.*; *Geo Abstr.*; *Mineral Abstr.*)

Zircon U-Pb age and Lu-Hf isotope constraints on Precambrian evolution of continental crust in the Songshan area, the south-central North China Craton J. Zhang, H.-F. Zhang and X.-X. Lu.....	1
The latest Neoproterozoic evolution of the Dunhuang block, eastern Tarim craton, northwestern China: Evidence from zircon U-Pb dating and Hf isotopic analyses J. Zhang, S. Yu, J. Gong, H. Li and K. Hou	21
Thermochronology of the Mont Laurier terrane, southern Canadian Grenville Province, and its bearing on defining orogenic architecture D.A. Schneider, N. Cope and D.K. Holm	43
Microfossil assemblage from the 3400 Ma Strelley Pool Formation in the Pilbara Craton, Western Australia: Results from a new locality K. Sugitani, K. Mimura, T. Nagaoka, K. Lepot and M. Takeuchi.....	59
Paleomagnetism of the Neoproterozoic diamictites of the Qiaobenbrak formation in the Aksu area, NW China: Constraints on the paleogeographic position of the Tarim Block B. Wen, Y.-X. Li and W. Zhu	75
Central/Eastern Indian Bundelkhand and Bastar cratons in the Palaeoproterozoic supercontinental reconstructions: A palaeomagnetic perspective T. Radhakrishna, R. Chandra, A.K. Srivastava and G. Balasubramanian.....	91
Recognition of Early and Late Neoproterozoic supracrustal units in West Africa and North-East Brazil from detrital zircon geochronology F. Kalsbeek, B.N. Ekwueme, J. Penaye, Z.S. de Souza and K. Thrahe	105
Siliciclastic associated banded iron formation from the 3.2 Ga Moodies Group, Barberton Greenstone Belt, South Africa T.R.R. Bontognali, W.W. Fischer and K.B. Föllmi	116
Problematic Mesoproterozoic fossil <i>Horodyskia</i> from Glacier National Park, Montana, USA G.J. Retallack, K.L. Dunn and J. Saxby	125
Tectonic model of the Limpopo belt: Constraints from magnetotelluric data D. Khoza, A.G. Jones, M.R. Muller, R.L. Evans, S.J. Webb and M. Miensopust, the SAMTEX team	143
Stress analysis, post-orogenic extension and 3.01 Ga gold mineralisation in the Barberton Greenstone Belt, South Africa R.H.G.M. Dirks, E.G. Charlesworth, M.R. Munyai and R. Wormald.....	157

CAPTION FOR COVER PHOTOGRAPH

3,243 million-year-old spherules in the Fig Tree Group, Barberton Greenstone Belt, South Africa, formed as a result of large meteorite impacts on the early Earth. The 35-cm-thick spherule bed (S3) is composed of nearly pure spherules produced during the condensation of an impact-produced rock vapor cloud. The estimated diameter of the bolide was 20–50 km. The spherules, 0.5–1.5 mm in diameter in the photo, include silica (clear), phyllosilicate (gray), and rutile/anatase-rich (black) varieties; massive and layered types; and a few originally hollow spherules. This is one of four spherule layers in the Barberton Belt, ranging from 3,470–3,243 Ma, that represent the oldest known impact deposits and provide direct evidence for a significant flux of large impactors as late as 3.2 Ga. Photograph: D.R. Lowe





ELSEVIER

Contents lists available at ScienceDirect

Precambrian Research

journal homepage: www.elsevier.com/locate/precambres

Contents

Special Issue

Precambrian Accretionary Orogens

Guest Editors:

M. Jayananda, M. Santosh, Bor-ming Jahn

Editorial

Precambrian accretionary orogens

M. Jayananda, M. Santosh and B.-m. Jahn 1

Research papers

The lower crust of the Dharwar Craton, Southern India: Patchwork of Archean granulitic domains
J.-J. Peucat, M. Jayananda, D. Chardon, R. Capdevila, C.M. Fanning and J.-L. Paquette 4

Paleoproterozoic accretionary orogenesis in the North China Craton: A SHRIMP zircon study
M. Santosh, D. Liu, Y. Shi and S.J. Liu 29

Neoarchean greenstone volcanism and continental growth, Dharwar craton, southern India: Constraints from SIMS U–Pb zircon geochronology and Nd isotopes
M. Jayananda, J.-J. Peucat, D. Chardon, B.K. Rao, C.M. Fanning and F. Corfu 55

The Murchison Greenstone Belt, South Africa: Accreted slivers with contrasting metamorphic conditions
S. Block, J.-F. Moyen, A. Zeh, M. Pujol, J. Jaguin and J.-L. Paquette 77

An appraisal of Archean supracrustal sequences in Chitradurga Schist Belt, Western Dharwar Craton, Southern India
T. Hokada, K. Horie, M. Satish-Kumar, Y. Ueno, A. Nasheeth, K. Mishima and K. Shiraishi 99

Crustal growth in the 3.4–2.7 Ga São José de Campestre Massif, Borborema Province, NE Brazil
E.L. Dantas, Z.S. de Souza, E. Wernick, P.C. Hackspacher, H. Martin, D. Xiaodong and J.-W. Li 120

Archean granitoid magmatism in the Canaã dos Carajás area: Implications for crustal evolution of the Carajás province, Amazonian craton, Brazil
G.R.L. Feio, R. Dall'Agnol, E.L. Dantas, M.J.B. Macambira, J.O.S. Santos, F.J. Althoff and J.E.B. Soares 157

Differentiation of the late-Archean sanukitoid series and some implications for crustal growth: Insights from geochemical modelling on the Bulai pluton, Central Limpopo Belt, South Africa
O. Laurent, R. Doucelance, H. Martin and J.-F. Moyen 186

Subduction related tectonic evolution of the Neoproterozoic eastern Dharwar Craton, southern India: New geochemical and isotopic constraints
M.R. Mohan, S.J. Piercey, B.S. Kamber and D.S. Sarma 204

Evolution of Archean crust in the Dharwar craton: The Nd isotope record
S. Dey 227

Tectonic evolution of the Eastern Ghats Belt, India
S. Dasgupta, S. Bose and K. Das 247

Chromite–silicate chemistry of the Neoproterozoic Sittampundi Complex, southern India: Implications for subduction-related arc magmatism
C.V. Dharma Rao, M. Santosh, K. Sajeew and B.F. Windley 259

Tectono-magmatic evolution of the Mesoproterozoic Singhora basin, central India: Evidence for compressional tectonics from structural data, AMS study and geochemistry of basic rocks S. Saha, K. Das, P.P. Chakraborty, P. Das, S. Karmakar and M.A. Mamtani	276
Geochemistry and neodymium model ages of Precambrian charnockites, Southern Granulite Terrain, India: Constraints on terrain assembly J.K. Tomson, Y.J. Bhaskar Rao, T. Vijaya Kumar and A.K. Choudhary	295
REE geochemistry of carbonates from the Guanmenshan Formation, Liaohe Group, NE Sino-Korean Craton: Implications for seawater compositional change during the Great Oxidation Event H.-S. Tang, Y.-J. Chen, M. Santosh, H. Zhong and T. Yang	316
Genesis of the 1.76 Ga Zhaiwa Mo-Cu and its link with the Xiong'er volcanics in the North China Craton: Implications for accretionary growth along the margin of the Columbia supercontinent X.H. Deng, Y.J. Chen, M. Santosh and J.M. Yao	337
Neoproterozoic plutonic rocks from the western Gyeonggi massif, South Korea: Implications for the amalgamation and break-up of the Rodinia supercontinent S.W. Kim, W.-S. Kee, S.R. Lee, M. Santosh and S. Kwon	349
Progressive accretionary tectonics of the Beishan orogenic collage, southern Altaids: Insights from zircon U-Pb and Hf isotopic data of high-grade complexes D. Song, W. Xiao, C. Han, J. Li, J. Qu, Q. Guo, L. Lin and Z. Wang	368
Petrology of the Neoproterozoic granulites from Central Dronning Maud Land, East Antarctica – Implications for southward extension of East African Orogen (EAO) N.C. Pant, A. Kundu, M.J. D'Souza and A. Saikia	389
High-Mg low-Ni olivine cumulates from a Pan-African accretionary belt in southern India: Implications for the genesis of volatile-rich high-Mg melts in suprasubduction setting V.J. Rajesh, S. Arai, M. Satish-kumar, M. Santosh and A. Tamura	409

(Abstracts/contents lists published in *Am. Geol. Inst. Bibliogr.*; *Abstr. Bull. Signalétique*; *Chem. Abstr.*; *Curr. Contents*; *Phys. Chem. Earth Sci.*; *Geo Abstr.*; *Mineral Abstr.*)

Paleoproterozoic collisional orogeny in Central Tianshan: Assembling the Tarim Block within the Columbia supercontinent X. Ma, L. Shu, M. Santosh and J. Li	1
A Sveconorwegian terrane boundary in the Caledonian Hardanger–Ryfylke Nappe Complex: The lost link between Telemarkia and the Western Gneiss Region? C. Roffeis, F. Corfu and R.H. Gabrielsen	20
Paleomagnetism of ca. 1.35 Ga sills in northern North China Craton and implications for paleogeographic reconstruction of the Mesoproterozoic supercontinent L. Chen, B. Huang, Z. Yi, J. Zhao and Y. Yan	36
⁴⁰ Ar/ ³⁹ Ar constraints on the age and thermal history of the Urucum Neoproterozoic banded iron-formation, Brazil T. Piacentini, P.M. Vasconcelos and K.A. Farley	48
Geochemistry of komatiites from the Tipasjärvi, Kuhmo, Suomussalmi, Ilomantsi and Tulppio greenstone belts, Finland: Implications for tectonic setting and Ni-sulphide prospectivity W.D. Maier, P. Peltonen, T. Halkoaho and E. Hänski	63
Carbon isotope records in a Mesoproterozoic epicratonic sea: Carbon cycling in a low-oxygen world G.J. Gilleaudeau and L.C. Kah	85
Late Paleoproterozoic multiple metamorphic events in the Quanji Massif: Links with Tarim and North China Cratons and implications for assembly of the Columbia supercontinent N. Chen, F. Liao, L. Wang, M. Santosh, M. Sun, Q. Wang and H.A. Mustafa	102
Contrasting types of Grenvillian granulite facies aluminous gneisses: Insights on protoliths and metamorphic events from zircon morphologies and ages S. Lasalle, C.M. Fisher, A. Indares and G. Dunning	117
Geochemical, geochronological and isotopic constraints on the origin of members of the allochthonous Shawanaga and basal Parry Sound domains, Central Gneiss Belt, Grenville Province, Ontario N.G. Culshaw, T. Slagstad, M. Raistrick and J. Dostal	131
Proterozoic ferroan feldspathic magmatism C.D. Frost and B.R. Frost	151
Paleomagnetism of ca. 2.3 Ga mafic dyke swarms in the northeastern Southern Granulite Terrain, India: Constraints on the position and extent of Dharwar craton in the Paleoproterozoic J.K. Dash, S.K. Pradhan, R. Bhutani, S. Balakrishnan, G. Chandrasekaran and N. Basavaiah	164
Tracking lateral $\delta^{13}\text{C}_{\text{carb}}$ variation in the Paleoproterozoic Pechenga Greenstone Belt, the north eastern Fennoscandian Shield P.E. Salminen, J.A. Karhu and V.A. Melezhik	177

(Contents continued on BM I)

CAPTION FOR COVER PHOTOGRAPH

3,243 million-year-old spherules in the Fig Tree Group, Barberton Greenstone Belt, South Africa, formed as a result of large meteorite impacts on the early Earth. The 35-cm-thick spherule bed (S3) is composed of nearly pure spherules produced during the condensation of an impact-produced rock vapor cloud. The estimated diameter of the bolide was 20–50 km. The spherules, 0.5–1.5 mm in diameter in the photo, include silica (clear), phyllosilicate (gray), and rutile/anatase-rich (black) varieties; massive and layered types; and a few originally hollow spherules. This is one of four spherule layers in the Barberton Belt, ranging from 3,470–3,243 Ma, that represent the oldest known impact deposits and provide direct evidence for a significant flux of large impactors as late as 3.2 Ga. Photograph: D.R. Lowe



(Contents continued from back cover)

New Mössbauer measurements of $\text{Fe}^{3+}/\Sigma\text{Fe}$ ratios in chromites from the early Proterozoic Bushveld Complex, South Africa J. Adetunji, S. Everitt and H. Rollinson	194
Mantle source, magma differentiation and sulfide saturation of the ~637 Ma Zhouan mafic-ultramafic intrusion in the northern margin of the Yangtze Block, Central China M. Wang, C.Y. Wang and Y. Sun	206
Nd isotope mapping of the Dysart gneiss complex: Evidence for a rifted block within the Central Metasedimentary Belt of the Grenville Province K. Moreton and A. P. Dickin	223
Neoproterozoic siliceous high-Mg basalt (SHMB) from the Taishan granite-greenstone terrane, Eastern North China Craton: Petrogenesis and tectonic implications T. Peng, S.A. Wilde, W. Fan and B. Peng	233
Neoproterozoic crustal recycling and mantle metasomatism: Hf-Nd-Pb-O isotope evidence from sanukitoids of the Fennoscandian shield E. Heilimo, J. Halla, T. Andersen and H. Huhma	250



Contents

Special Issue

Evolving Early Earth

Guest Editors:

Steve Beresford, Ian Tyler, Hugh Smithies

Editorial

Preface	
S. Beresford, I. Tyler and H. Smithies	1
Research papers	
A critical assessment of Neoproterozoic "plume only" geodynamics: Evidence from the Superior Province	
D.A. Wyman	3
The hunting of the snArc	
J.H. Bédard, L.B. Harris and P.C. Thurston	20
Long-lived, autochthonous development of the Archean Murchison Domain, and implications for Yilgarn Craton tectonics	
M.J. Van Kranendonk, T.J. Ivanic, M.T.D. Wingate, C.L. Kirkland and S. Wyche	49
Archean gravity-driven tectonics on hot and flooded continents: Controls on long-lived mineralised hydrothermal systems away from continental margins	
N. Thébaud and P.F. Rey	93
Zircon geochronology of late Archean komatiitic sills and their felsic country rocks, south-central Zimbabwe: A revised age for the Reliance komatiitic event and its implications	
M.D. Prendergast and M.T.D. Wingate	105
Imaging Archean-age whole mineral systems	
D.B. Snyder	125
Were intercalated komatiites and dacites at the Black Swan nickel sulphide mine, Yilgarn Craton, Western Australia, emplaced as extrusive lavas or intrusive bodies? The significance of breccia textures and contact relationships	
R.A.F. Cas, K. Marks, S. Perazzo, S.W. Beresford, J. Trofimovs and N. Rosengren	133
Petrology and geochemistry of the ~2.9 Ga Itilliarsuk banded iron formation and associated supracrustal rocks, West Greenland: Source characteristics and depositional environment	
R. Haugaard, R. Frei, H. Stendal and K. Konhauser	150
The evolution of the $^{87}\text{Sr}/^{86}\text{Sr}$ of marine carbonates does not constrain continental growth	
N. Flament, N. Coltice and P.F. Rey	177
How many arcs can dance on the head of a plume? A 'Comment' on: A critical assessment of Neoproterozoic 'plume only' geodynamics: Evidence from the Superior province, by Derek Wyman, Precambrian Research, 2012	
J.H. Bédard	189
A reply to "How many arcs can dance on the head of a plume?" by Jean Bédard, Precambrian Research, 2012	
D.A. Wyman	198

(Abstracts/contents lists published in *Am. Geol. Inst. Bibliogr.*; *Abstr. Bull. Signalétique*; *Chem. Abstr.*; *Curr. Contents*; *Phys. Chem. Earth Sci.*, *Geo Abstr.*; *Mineral Abstr.*)

U–Pb geochronology of the granite magmatism in the Embu Terrane: Implications for the evolution of the Central Ribeira Belt, SE Brazil A. Alves, V.d.A. Janasi, M.d.C. Campos Neto, L. Heaman and A. Simonetti	1
Continental origin of eclogites in the North Qinling terrane and its tectonic implications H. Wang, Y.-B. Wu, S. Gao, X.-C. Liu, Q. Liu, Z.-W. Qin, S.-W. Xie, L. Zhou and S.-H. Yang	13
Zircon U–Pb dating and Hf isotope analysis on the Taihua Complex: Constraints on the formation and evolution of the Trans-North China Orogen X. Yu, J. Liu, C. Li, S. Chen and Y. Dai	31
The Paleoproterozoic Waterberg Group, South Africa: Provenance and its relation to the timing of the Limpopo orogeny P.L. Corcoran, A.J. Bumby and D.W. Davis	45
Zircon U–Pb ages, trace elements and Nd–Hf isotopic geochemistry of Guyang sanukitoids and related rocks: Implications for the Archean crustal evolution of the Yinshan Block, North China Craton X. Ma, J. Guo, F. Liu, Q. Qian and H. Fan	61
Petrographic, geochemical and SHRIMP U–Pb titanite age characterization of the Thabazimbi mafic sills: Extended time frame and a unifying petrogenetic model for the Bushveld Large Igneous Province H.M. Rajesh, B.C. Chisonga, K. Shindo, N.J. Beukes and R.A. Armstrong	79
Mesoproterozoic intraplate magmatic ‘barcode’ record of the Angola portion of the Congo Craton: Newly dated magmatic events at 1505 and 1110 Ma and implications for Nuna (Columbia) supercontinent reconstructions R.E. Ernst, E. Pereira, M.A. Hamilton, S.A. Pisarevsky, J. Rodrigues, C.C.G. Tassinari, W. Teixeira and V. Van-Dunem	103
Geochemistry and petrogenesis of Proterozoic mafic rocks from East Khasi Hills, Shillong Plateau, Northeastern India J. Ray, A. Saha, C. Koeberl, M. Thoni, S. Ganguly and S. Hazra	119
Neoproterozoic low to negative $\delta^{18}\text{O}$ volcanic and intrusive rocks in the Qinling Mountains and their geological significance J. Liu and L. Zhang	138
Mo isotopic composition of the mid-Neoproterozoic ocean: An iron formation perspective G.J. Baldwin, T.F. Nägler, N.D. Greber, E.C. Turner and B.S. Kamber	168
Geochemistry and tectonic implications of late Mesoproterozoic alkaline bimodal volcanic rocks from the Tieshajie Group in the southeastern Yangtze Block, South China L. Li, S. Lin, G. Xing, D.W. Davis, W.J. Davis, W. Xiao and C. Yin	179
Provenance and ages of the Altyn Complex in Altyn Tagh: Implications for the early Neoproterozoic evolution of northwestern China C. Wang, L. Liu, W.-Q. Yang, X.-H. Zhu, Y.-T. Cao, L. Kang, S.-F. Chen, R.-S. Li and S.-P. He	193

(Contents continued on BM I)

CAPTION FOR COVER PHOTOGRAPH

3,243 million-year-old spherules in the Fig Tree Group, Barberton Greenstone Belt, South Africa, formed as a result of large meteorite impacts on the early Earth. The 35-cm-thick spherule bed (S3) is composed of nearly pure spherules produced during the condensation of an impact-produced rock vapor cloud. The estimated diameter of the bolide was 20–50 km. The spherules, 0.5–1.5 mm in diameter in the photo, include silica-(clear), phyllosilicate- (gray), and rutile/anatase-rich (black) varieties; massive and layered types; and a few originally hollow spherules. This is one of four spherule layers in the Barberton Belt, ranging from 3,470–3,243 Ma, that represent the oldest known impact deposits and provide direct evidence for a significant flux of large impactors as late as 3.2 Ga. Photograph: D.R. Lowe



(Contents continued from back cover)

LA-ICP-MS dating of zircons from Meso- and Neoproterozoic granitoids of the Pietersburg block (South Africa): Crustal evolution at the northern margin of the Kaapvaal craton
 O. Laurent, J.-L. Paquette, H. Martin, R. Doucelance and J.-F. Moyen 209

Age, origin and significance of nodular sulfides in 2680 Ma carbonaceous black shale of the Eastern Goldfields Superterrane, Yilgarn Craton, Western Australia
 J.A. Steadman, R.R. Large, S. Meffre and S.W. Bull 227

Discussion of Saha et al. (2012, Precambrian Research) Tectono-magmatic evolution of the Mesoproterozoic Singhora basin, central India: Evidence for compressional tectonics from structural data, AMS study and geochemistry of basic rocks
 G.K. Deb..... 248

(Abstracts/contents lists published in *Am. Geol. Inst. Bibliogr.*; *Abstr. Bull. Signalétique*; *Chem. Abstr.*; *Curr. Contents*; *Phys. Chem. Earth Sci.*; *Geo Abstr.*; *Mineral Abstr.*)

Zircon U–Pb ages and Lu–Hf isotopes of Paleoproterozoic metasedimentary rocks in the Korla Complex, NW China: Implications for metamorphic zircon formation and geological evolution of the Tarim Craton R. Ge, W. Zhu, H. Wu, J. He and B. Zheng	1
Tectonic evolution of the Qinling orogenic belt, Central China: New evidence from geochemical, zircon U–Pb geochronology and Hf isotopes Y. Shi, J.-H. Yu and M. Santosh	19
Late Paleoproterozoic sedimentary and mafic rocks in the Hekou area, SW China: Implication for the reconstruction of the Yangtze Block in Columbia W.T. Chen, M.-F. Zhou and X.-F. Zhao.....	61
Basin analysis in polymetamorphic terranes: An example from east Antarctica J.A. Halpin, N.R. Daczko, G.L. Clarke and K.R. Murray	78
Palaeoproterozoic terrestrial sedimentation in the Beasley River Quartzite, lower Wyloo Group, Western Australia R. Mazumder and M.J. Van Kranendonk	98
Paleoarchean partial convective overturn in the Singhbhum Craton, Eastern India N. Prabhakar and A. Bhattacharya	106
Explaining the exceptional preservation of Ediacaran rangeomorphs from Spaniard's Bay, Newfoundland: A hydraulic model M.D. Brasier, A.G. Liu, L. Menon, J.J. Matthews, D. McIlroy and D. Wacey	122
Timing and mechanisms of multiple episodes of migmatization in the Korla Complex, northern Tarim Craton, NW China: Constraints from zircon U–Pb–Lu–Hf isotopes and implications for crustal growth R. Ge, W. Zhu, H. Wu, B. Zheng and J. He	136
The ancestry and magmatic evolution of Archaean TTG rocks of the Quadrilátero Ferrífero province, southeast Brazil C. Lana, F.F. Alkmim, R. Armstrong, R. Scholz, R. Romano and H.A. Nalini Jr.	157
Lithogeochemistry, geochronology and geodynamic setting of the Lupa Terrane, Tanzania: Implications for the extent of the Archean Tanzanian Craton C.J.M. Lawley, D. Selby, D.J. Condon, M. Horstwood, I. Millar, Q. Crowley and J. Imber	174
U–Pb systematics in carbonates of the Postmasburg Group, Transvaal Supergroup, South Africa: Primary <i>versus</i> metasomatic controls B. Fairey, H. Tsikos, F. Corfu and S. Polteau	194
Constraints from experimental melting of amphibolite on the depth of formation of garnet-rich restites, and implications for models of Early Archean crustal growth C. Zhang, F. Holtz, J. Koepke, P.E. Wolff, C. Ma and J.H. Bédard	206
A new lithostratigraphic subdivision and geodynamic model for the Pan-African western Saldania Belt, South Africa H.E. Frimmel, M.A.S. Basei, V.X. Correa and N. Mbangula	218

(Contents continued on BM I)

CAPTION FOR COVER PHOTOGRAPH

3,243 million-year-old spherules in the Fig Tree Group, Barberton Greenstone Belt, South Africa, formed as a result of large meteorite impacts on the early Earth. The 35-cm-thick spherule bed (S3) is composed of nearly pure spherules produced during the condensation of an impact-produced rock vapor cloud. The estimated diameter of the bolide was 20–50 km. The spherules, 0.5–1.5 mm in diameter in the photo, include silica-(clear), phyllosilicate- (gray), and rutile/anatase-rich (black) varieties; massive and layered types; and a few originally hollow spherules. This is one of four spherule layers in the Barberton Belt, ranging from 3,470–3,243 Ma, that represent the oldest known impact deposits and provide direct evidence for a significant flux of large impactors as late as 3.2 Ga. Photograph: D.R. Lowe



(Contents continued from back cover)

Timing of deposition and deformation of the Moodies Group (Barberton Greenstone Belt, South Africa): Very-high-resolution of Archaean surface processes C. Heubeck, J. Engelhardt, G.R. Byerly, A. Zeh, B. Sell, T. Luber and D.R. Lowe	236
The lithospheric mantle underneath the Gibeon Kimberlite field (Namibia): A mix of old and young components— Evidence from Lu–Hf and Sm–Nd isotope systematics T. Luchs, G.P. Brey, A. Gerdes and H.E. Höfer	263
Seismic imaging of the Proterozoic Cuddapah basin, south India and regional geodynamics K. Chandrakala, D.M. Mall, D. Sarkar and O.P. Pandey	277
A petrographic and isotopic criterion of the state of preservation of Precambrian cherts based on the characterization of the quartz veins J. Marin-Carbonne, F. Faure, M. Chaussidon, D. Jacob and F. Robert	290
Suprasubduction zone ophiolite from Agali hill: Petrology, zircon SHRIMP U–Pb geochronology, geochemistry and implications for Neoproterozoic plate tectonics in southern India M. Santosh, E. Shaji, T. Tsunogae, M.R. Mohan, M. Satyanarayanan and K. Horie	301
Early Neoproterozoic (~850 Ma) back-arc basin in the Central Jiangnan Orogen (Eastern South China): Geochronological and petrogenetic constraints from meta-basalts Y. Zhang, Y. Wang, H. Geng, Y. Zhang, W. Fan and H. Zhong	325
Geochronological, geochemical and Nd–Hf–O ₃ isotopic fingerprinting of an early Neoproterozoic arc–back-arc system in South China and its accretionary assembly along the margin of Rodinia Y. Wang, A. Zhang, P.A. Cawood, W. Fan, J. Xu, G. Zhang and Y. Zhang	343
Paleomagnetism of Cryogenian Kitoi mafic dykes in South Siberia: Implications for Neoproterozoic paleogeography S.A. Pisarevsky, D.P. Gladkochub, K.M. Konstantinov, A.M. Mazukabzov, A.M. Stanevich, J.B. Murphy, J.A. Tait, T.V. Donskaya and I.K. Konstantinov	372
Comment on “Trace fossil evidence for Ediacaran bilaterian animals with complex behaviors” by Chen et al. [Precambrian Res. 224 (2013) 690–701] G.J. Retallack	383
Reply to comment on “Trace fossil evidence for Ediacaran bilaterian animals with complex behaviors” [Precambrian Res. 224 (2013) 690–701] Z. Chen, C. Zhou, M. Meyer, K. Xiang, J.D. Schiffbauer, X. Yuan and S. Xiao	386
Stable isotope (S, C) chemostratigraphy and hydrocarbon biomarkers in the Ediacaran upper section of Sierras Bayas Group, Argentina M. Bagnoud-Velásquez, J.E. Spangenberg, D.G. Poiré and L.E.G. Peral	388
Photoelectrons from minerals and microbial world: A perspective on life evolution in the early Earth A. Lu, Y. Li, X. Wang, H. Ding, C. Zeng, X. Yang, R. Hao, C. Wang and M. Santosh	401
Using detrital zircon ages and Hf isotopes to identify 1.48–1.45 Ga sedimentary basins and fingerprint sources of exotic 1.6–1.5 Ga grains in southwestern Laurentia M.F. Doe, J.V. Jones III, K.E. Karlstrom, B. Dixon, G. Gehrels and M. Pecha	409



Contents

Special Issue

Paleoproterozoic tectonic assembly of the western Canadian shield: new findings and implications for the reconstruction of Laurentia/Nuna

Guest Editors:

Robert G. Berman, Kathryn M. Bethune

Editorial

Paleoproterozoic tectonic assembly of the western Canadian shield: New findings and implications for paleocontinental reconstruction

R.G. Berman and K.M. Bethune 1

Research Papers

A domain-based digital summary of the evolution of the Palaeoproterozoic of North America and Greenland and associated unconformity-related uranium mineralization

B.M. Eglington, S.J. Pehrsson, K.M. Ansdell, J.-L. Lescuyer, D. Quirt, J.-P. Milesi and P. Brown 4

Two Neoproterozoic supercontinents revisited: The case for a Rae family of cratons

S.J. Pehrsson, R.G. Berman, B. Eglington and R. Rainbird 27

The Arrowsmith orogeny: Geochronological and thermobarometric constraints on its extent and tectonic setting in the Rae craton, with implications for pre-Nuna supercontinent reconstruction

R.G. Berman, S. Pehrsson, W.J. Davis, J.J. Ryan, H. Qui and K.E. Ashton 44

New depositional age constraints for the Murmac Bay group of the southern Rae craton, Canada

K.E. Ashton, R.P. Hartlaub, K.M. Bethune, L.M. Heaman, N. Rayner and G.R. Niebergall 70

Structural, petrological and U-Pb SHRIMP geochronological study of the western Beaverlodge domain: Implications for crustal architecture, multi-stage orogenesis and the extent of the Taltson orogen in the SW Rae craton, Canadian Shield

K.M. Bethune, R.G. Berman, N. Rayner and K.E. Ashton 89

The Paleoproterozoic Kaminak dykes, Hearne craton, western Churchill Province, Nunavut, Canada: Preliminary constraints on their age and petrogenesis

H.A. Sandeman, L.M. Heaman and A.N. LeCheminant 119

The tectonometamorphic evolution of Southampton Island, Nunavut: Insight from petrologic modeling and in situ SHRIMP geochronology of multiple episodes of monazite growth

R.G. Berman, M. Sanborn-Barrie, N. Rayner and J. Whalen 140

Paleoproterozoic orogenesis during *Nuna* aggregation: A case study of reworking of the Rae craton, Woodburn Lake, Nunavut

S.J. Pehrsson, R.G. Berman and W.J. Davis 167

Seismic anisotropy and mantle structure of the Rae craton, central Canada, from joint interpretation of SKS splitting and receiver functions

D.B. Snyder, R.G. Berman, J.-M. Kendall and M. Sanborn-Barrie 189

Sequence stratigraphy, provenance, C and O isotopic composition, and correlation of the late Paleoproterozoic-early Mesoproterozoic upper Hornby Bay and lower Dismal Lakes groups, NWT and Nunavut

K. Hahn, R. Rainbird and B. Cousens 209

(Abstracts/contents lists published in *Am. Geol. Inst. Bibliogr.*; *Abstr. Bull. Signalétique*; *Chem. Abstr.*; *Curr. Contents*; *Phys. Chem. Earth Sci.*; *Geo Abstr.*; *Mineral Abstr.*)

New U-Pb age constraints for the Laxford Shear Zone, NW Scotland: Evidence for tectono-magmatic processes associated with the formation of a Paleoproterozoic supercontinent K.M. Goodenough, O.G. Crowley, M. Krabbendam and S.F. Parry	1
Juvenile crust formation in the northeastern Kaapvaal Craton at 2.97 Ga—Implications for Archean terrane accretion, and the source of the Pietersburg gold A. Zeh, J. Jaguin, M. Poujol, P. Boulvais, S. Block and J.-L. Paquette	20
Wrench-shearing during the Namaqua Orogenesis—Mesoproterozoic late stage deformation effects during Rodinia assembly W.P. Colliston and A.E. Schoch	44
Microstructures in metasedimentary rocks from the Neoproterozoic Bonahaven Formation, Scotland: Microconcretions, impact spherules, or microfossils? R.P. Anderson, I.J. Fairchild, N.J. Tosca and A.H. Knoll	59
Microbially induced sedimentary structures from the Mesoproterozoic Huangqikou Formation, Helan Mountain region, northern China Z.-W. Lan, Z.-Q. Chen, X.-H. Li and K. Kaiho	73
Neoproterozoic high-K granites produced by melting of newly formed mafic crust in the Huangling region, South China J.-H. Zhao, M.-F. Zhou and J.-P. Zheng	93
Depositional history of the Upper Vindhyan succession, central India: Time constraints from Pb-Pb isochron ages of its carbonate components K. Gopalan, A. Kumar, S. Kumar and B. Vijayagopal	108
Geochronology and paleoenvironment of the pre-Sturtian glacial strata: Evidence from the Liantuo Formation in the Nanhua rift basin of the Yangtze Block, South China Q. Du, Z. Wang, J. Wang, Y. Qiu, X. Jiang, Q. Deng and F. Yang	118
The Suursaari conglomerate (SE Fennoscandian shield; Russia)—Indication of cratonic conditions and rapid reworking of quartz arenitic cover at the outset of the emplacement of the rapakivi granites at ca. 1.65 Ga J. Pokki, J. Kohonen, O.T. Rämö and T. Andersen	132
Age, petrogenesis and tectonic setting of the Thessalon volcanic rocks, Huronian Supergroup, Canada K.Y. Ketchum, L.M. Heaman, G. Bennett and D.J. Hughes	144
Highly depleted harzburgite-dunite-chromitite complexes from the Neoproterozoic ophiolite, south Eastern Desert, Egypt: A possible recycled upper mantle lithosphere A.H. Ahmed	173
Neoproterozoic high-Mg basalts formed by melting of ambient mantle in South China J.-H. Zhao and M.-F. Zhou	193

(Contents continued on BM I)

CAPTION FOR COVER PHOTOGRAPH

3,243 million-year-old spherules in the Fig Tree Group, Barberton Greenstone Belt, South Africa, formed as a result of large meteorite impacts on the early Earth. The 35-cm-thick spherule bed (S3) is composed of nearly pure spherules produced during the condensation of an impact-produced rock vapor cloud. The estimated diameter of the bolide was 20–50 km. The spherules, 0.5–1.5 mm in diameter in the photo, include silica-(clear), phyllosilicate- (gray), and rutile/anatase-rich (black) varieties; massive and layered types; and a few originally hollow spherules. This is one of four spherule layers in the Barberton Belt, ranging from 3,470–3,243 Ma, that represent the oldest known impact deposits and provide direct evidence for a significant flux of large impactors as late as 3.2 Ga. Photograph: D.R. Lowe



(Contents continued from back cover)

Lu-Hf isotope evidence for Paleoproterozoic metamorphism and deformation of Archean oceanic crust along the Dharwar Craton margin, southern India N.M. Noack, R. Kleinschrodt, M. Kirchenbaur, R.O.C. Fonseca and C. Münker	206
Unraveling the Precambrian crustal evolution by Neoproterozoic conglomerates, Jiangnan orogen: U-Pb and Hf isotopes of detrital zircons D. Wang, X.-L. Wang, J.-C. Zhou and X.-J. Shu	223
Petrogenesis, <i>P-T-t</i> path, and tectonic significance of high-pressure mafic granulites from the Jiaobei terrane, North China Craton P. Liu, F. Liu, C. Liu, F. Wang, J. Liu, H. Yang, J. Cai and J. Shi	237
Geology of the Monapo Klippe, NE Mozambique and its significance for assembly of central Gondwana P.H. Macey, J.A. Miller, C.D. Rowe, G.H. Grantham, P. Siegfried, R.A. Armstrong, J. Kemp and J. Bacalau	259
Metamorphic P-T paths and New Zircon U-Pb age data for garnet-mica schist from the Wutai Group, North China Craton J. Qian, C. Wei, X. Zhou and Y. Zhang	282
Zircon U-Pb and Lu-Hf isotopic and whole-rock geochemical constraints on the protolith and tectonic history of the Changhai metamorphic supracrustal sequence in the Jiao-Liao-Ji Belt, southeast Liaoning Province, northeast China E. Meng, F.-L. Liu, Y. Cui and J. Cai	297
Meso/Neoarchean crustal domains along the north Konkan coast, western India: The Western Dharwar Craton and the Antongil-Masora Block (NE Madagascar) connection S. Rekha, T.A. Viswanath, A. Bhattacharya and N. Prabhakar	316
Episodic crustal growth in the southern segment of the Trans-North China Orogen across the Archean-Proterozoic boundary X.-L. Huang, S.A. Wilde and J.-W. Zhong	337
Thermal transport properties of major Archean rock types to high temperature and implications for cratonic geotherms J.D. Merriman, A.G. Whittington, A.M. Hofmeister, P.I. Nabelek and K. Benn	358



Contents

Special Issue

Crossing of Neoproterozoic orogens

Guest Editors:

M. Satish-Kumar, Tomokazu Hokada

Editorial

Neoproterozoic orogens amalgamating East Gondwana: Did they cross each other?

M. Satish-Kumar, T. Hokada, M. Owada, Y. Osanai and K. Shiraishi 1

Research Papers

Geologic evolution of the Sør Rondane Mountains, East Antarctica: Collision tectonics proposed based on metamorphic processes and magnetic anomalies

Y. Osanai, Y. Nogi, S. Baba, N. Nakano, T. Adachi, T. Hokada, T. Toyoshima, M. Owada, M. Satish-Kumar, A. Kamei and I. Kitano 8

Sinistral transpressional and extensional tectonics in Dronning Maud Land, East Antarctica, including the Sør Rondane Mountains

T. Toyoshima, Y. Osanai, S. Baba, T. Hokada, N. Nakano, T. Adachi, M. Otsubo, M. Ishikawa and Y. Nogi 30

Late Proterozoic juvenile arc metatonalite and adakitic intrusions in the Sør Rondane Mountains, eastern Dronning Maud Land, Antarctica

A. Kamei, K. Horie, M. Owada, M. Yuhara, N. Nakano, Y. Osanai, T. Adachi, Y. Hara, M. Terao, S. Teuchi, T. Shimura, K. Tsukada, T. Hokada, C. Iwata, K. Shiraishi, H. Ishizuka and Y. Takahashi 47

Magmatic history and evolution of continental lithosphere of the Sør Rondane Mountains, eastern Dronning Maud Land, East Antarctica

M. Owada, A. Kamei, K. Horie, T. Shimura, M. Yuhara, K. Tsukada, Y. Osanai and S. Baba 63

Comparison of the metamorphic history of the Monapo Complex, northern Mozambique and Balchenfjella and Austhameren areas, Sør Rondane, Antarctica: Implications for the Kuunga Orogeny and the amalgamation of N and S Gondwana

G.H. Grantham, P.H. Macey, K. Horie, T. Kawakami, M. Ishikawa, M. Satish-Kumar, N. Tsuchiya, P. Graser and S. Azevedo 85

Timing of metamorphism in the central Sør Rondane Mountains, eastern Dronning Maud Land, East Antarctica: Constrains from SHRIMP zircon and EPMA monazite dating

T. Adachi, Y. Osanai, T. Hokada, N. Nakano, S. Baba and T. Toyoshima 136

Multiple thermal events recorded in metamorphosed carbonate and associated rocks from the southern Austkampane region in the Sør Rondane Mountains, East Antarctica: A protracted Neoproterozoic history at the Gondwana suture zone

N. Nakano, Y. Osanai, A. Kamei, M. Satish-Kumar, T. Adachi, T. Hokada, S. Baba and T. Toyoshima 161

Unraveling the metamorphic history at the crossing of Neoproterozoic orogens, Sør Rondane Mountains, East Antarctica: Constraints from U-Th-Pb geochronology, petrography, and REE geochemistry

T. Hokada, K. Horie, T. Adachi, Y. Osanai, N. Nakano, S. Baba and T. Toyoshima 183

Counterclockwise *P-T* path and isobaric cooling of metapelites from Brattnipene, Sør Rondane Mountains, East Antarctica: Implications for a tectonothermal event at the proto-Gondwana margin

S. Baba, Y. Osanai, N. Nakano, M. Owada, T. Hokada, K. Horie, T. Adachi and T. Toyoshima 210

Chlorine-rich fluid or melt activity during granulite facies metamorphism in the Late Proterozoic to Cambrian continental collision zone—An example from the Sør Rondane Mountains, East Antarctica F. Higashino, T. Kawakami, M. Satish-Kumar, M. Ishikawa, K. Maki, N. Tsuchiya, G.H. Grantham and T. Hirata	229
Late Neoproterozoic extensional detachment in eastern Sør Rondane Mountains, East Antarctica: Implications for the collapse of the East African Antarctic Orogen M. Ishikawa, T. Kawakami, M. Satish-Kumar, G.H. Grantham, Y. Hōkazono, M. Saso and N. Tsuchiya	247
Late-Tonian to early-Cryogenian apparent depositional ages for metacarbonate rocks from the Sør Rondane Mountains, East Antarctica N. Otsuji, M. Satish-Kumar, A. Kamei, N. Tsuchiya, T. Kawakami, M. Ishikawa and G.H. Grantham	257
Geological structures inferred from airborne geophysical surveys around Lützow-Holm Bay, East Antarctica Y. Nogi, W. Jokat, K. Kitada and D. Steinhage	279
Age, Nd-Hf isotopes, and geochemistry of the Vijayan Complex of eastern and southern Sri Lanka: A Grenville-age magmatic arc of unknown derivation A. Kröner, Y. Rojas-Agramonte, K.V.W. Kehelpannala, T. Zack, E. Hegner, H.Y. Geng, J. Wong and M. Barth	288
How long-lived is ultrahigh temperature (UHT) metamorphism? Constraints from zircon and monazite geochronology in the Eastern Ghats orogenic belt, India F.J. Korhonen, C. Clark, M. Brown, S. Bhattacharya and R. Taylor	322

(Abstracts/contents lists published in *Am. Geol. Inst. Bibliogr.*; *Abstr. Bull. Signalétique*; *Chem. Abstr.*; *Curr. Contents*; *Phys. Chem. Earth Sci.*; *Geo Abstr.*; *Mineral Abstr.*)

Detrital zircon record of Neoproterozoic active-margin sedimentation in the eastern Jiangnan Orogen, South China W. Wang, M.-F. Zhou, D.-P. Yan, L. Li and J. Malpas	1
Terminal Proterozoic cyanobacterial blooms and phosphogenesis documented by the Doushantuo granular phosphorites I: <i>In situ</i> micro-analysis of textures and composition Z. She, P. Strother, G. McMahon, L.R. Nittler, J. Wang, J. Zhang, L. Sang, C. Ma and D. Papineau	20
Neoproterozoic-Paleoproterozoic multiple tectonothermal events in the western Alxa block, North China Craton and their geological implication: Evidence from zircon U-Pb ages and Hf isotopic composition J. Zhang, J. Gong, S. Yu, H. Li and K. Hou	36
New evidences for sedimentary attributes and timing of the "Macaoyuan conglomerates" on the northern margin of the Yangtze block in southern China J. Wang, Qi. Deng, Z.-j. Wang, Y.-s. Qiu, T.-z. Duan, X.-s. Jiang and Q.-x. Yang	58
Problematic urn-shaped fossils from a Paleoproterozoic (2.2 Ga) paleosol in South Africa G.J. Retallack, E.S. Krull, G.D. Thackray and D. Parkinson	71
Iron isotopic constraints on the genesis of Bayan Obo ore deposit, Inner Mongolia, China J. Sun, X. Zhu, Y. Chen and N. Fang	88
Plate margin paleostress variations and intracontinental deformations in the evolution of the Cuddapah basin through Proterozoic V. Tripathy and D. Saha	107
Not-so-suspect terrane: Constraints on the crustal evolution of the Rudall Province C.L. Kirkland, S.P. Johnson, R.H. Smithies, J.A. Hollis, M.T.D. Wingate, I.M. Tyler, A.H. Hickman, J.B. Cliff, S. Tesselina, E.A. Belousova and R.C. Murphy	131
Tectonic framework and crustal evolution of the Precambrian basement of the Tarim Block in NW China: New geochronological evidence from deep drilling samples Z.-Q. Xu, B.-Z. He, C.-L. Zhang, J.-X. Zhang, Z.-M. Wang and Z.-H. Cai	150
The Neoproterozoic granitoids from the Qilian block, NW China: Evidence for a link between the Qilian and South China blocks K.-a. Tung, H.-y. Yang, D.-y. Liu, J.-x. Zhang, H.-j. Yang, Y.-h. Shau and C.-y. Tseng	163
Mesoproterozoic high Fe-Ti mafic magmatism in western Shandong, North China Craton: Petrogenesis and implications for the final breakup of the Columbia supercontinent T. Peng, S.A. Wilde, W. Fan, B. Peng and Y. Mao	190
⁴⁰ Ar ³⁹ Ar thermochronology of Paleoproterozoic granitoids of northeast Burkina Faso, West African Craton: Implications for regional tectonics B. Tapsoba, C.-H. Lo, U. Wenmenga, B.-M. Jahn and S.-L. Chung	208

(Contents continued on BM I)

CAPTION FOR COVER PHOTOGRAPH

3,243 million-year-old spherules in the Fig Tree Group, Barberton Greenstone Belt, South Africa, formed as a result of large meteorite impacts on the early Earth. The 35-cm-thick spherule bed (S3) is composed of nearly pure spherules produced during the condensation of an impact-produced rock vapor cloud. The estimated diameter of the bolide was 20–50 km. The spherules, 0.5–1.5 mm in diameter in the photo, include silica-(clear), phyllosilicate- (gray), and rutile/anatase-rich (black) varieties; massive and layered types; and a few originally hollow spherules. This is one of four spherule layers in the Barberton Belt, ranging from 3,470–3,243 Ma, that represent the oldest known impact deposits and provide direct evidence for a significant flux of large impactors as late as 3.2 Ga. Photograph: D.R. Lowe



(Contents continued from outside back cover)

U-Pb dating and Hf isotope study of detrital zircons from the Zhifu Group, Jiaobei Terrane, North China Craton: Provenance and implications for Precambrian crustal growth and recycling J. Liu, F. Liu, Z. Ding, H. Yang, C. Liu, P. Liu, L. Xiao, L. Zhao and J. Geng	230
The generation and evolution of Archean continental crust in the Dunhuang block, northeastern Tarim craton, northwestern China K. Zong, Y. Liu, Z. Zhang, Z. He, Z. Hu, J. Guo and K. Chen	251
New U-Pb geochronology from Timiskaming-type assemblages in the Shebandowan and Vermilion greenstone belts, Wawa subprovince, Superior Craton: Implications for the Neoproterozoic development of the southwestern Superior Province R.W.D. Lodge, H.L. Gibson, G.M. Stott, G.J. Hudak, M.A. Jirsa and M.A. Hamilton	264
Earth's earliest global glaciation? Carbonate geochemistry and geochronology of the Polisarka Sedimentary Formation, Kola Peninsula, Russia A.T. Brasier, A.P. Martin, V.A. Melezhik, A.R. Prave, D.J. Condon and A.E. Fallick, FAR-DEEP Scientists	278
Discovery of an Eo-Meso-Neoproterozoic terrane in the East Greenland Caledonides S.M. Johnston and A.R.C. Kylander-Clark	295

(Abstracts/contents lists published in *Am. Geol. Inst. Bibliogr.*; *Abstr. Bull. Signalétique*; *Chem. Abstr.*; *Curr. Contents*; *Phys. Chem. Earth Sci.*; *Geo Abstr.*; *Mineral Abstr.*)

Archaean andesite petrogenesis: Insights from the Grædefjord Supracrustal Belt, southern West Greenland K. Szilas, J.E. Hoffmann, A. Scherstén, T.F. Kokfelt and C. Münker	1
Paleogeography of Baltica in the Ediacaran: Paleomagnetic and geochronological data from the clastic Zigan Formation, South Urals N.M. Levashova, M.L. Bazhenov, J.G. Meert, N.B. Kuznetsov, I.V. Golovanova, K.N. Danukalov and N.M. Fedorova	16
Mesoproterozoic subduction under the eastern edge of the Kalahari-Grunehogna Craton preceding Rodinia assembly: The Ritscherflya detrital zircon record, Ahlmannryggen (Dronning Maud Land, Antarctica) H.R. Marschall, C.J. Hawkesworth and P.T. Leat	31
Geochronology and geochemistry of Mesoproterozoic granitoids in the Lhasa terrane, south Tibet: Implications for the early evolution of Lhasa terrane W.-C. Xu, H.-F. Zhang, N. Harris, L. Guo, F.-B. Pan and S. Wang	46
Decrease of seawater CO ₂ concentration in the Late Archean: An implication from 2.6 Ga seafloor hydrothermal alteration T. Shibuya, M. Tahata, Y. Ueno, T. Komiya, K. Takai, N. Yoshida, S. Maruyama and M.J. Russell	59
Sequence stratigraphy and formalization of the Middle Uinta Mountain Group (Neoproterozoic), central Uinta Mountains, Utah: A closer look at the western Laurentian Seaway at ca. 750 Ma E.M. Kingsbury-Stewart, S.L. Osterhout, P.K. Link and C.M. Dehler	65
U-Pb dating constraints on the felsic and intermediate volcanic sequence of the nickel-sulphide bearing Cosmos succession, Agnew-Wiluna greenstone belt, Yilgarn Craton, Western Australia A. de Joux, T. Thordarson, M. Denny, R.W. Hinton and A.J. de Joux	85
The 1750 Ma Magmatic Event of the West African Craton (Anti-Atlas, Morocco) N. Youbi, D. Kouyaté, U. Söderlund, R.E. Ernst, A. Soulimani, A. Hafid, M. Ikenne, A. El Bahat, H. Bertrand, K. Rkha Chaham, M. Ben Abbou, A. Mortaji, M. El Ghorfi, M. Zouhair and M. El Janati	106
Constraining the depositional history of the Neoproterozoic Shaler Supergroup, Amundsen Basin, NW Canada: Rhenium-osmium dating of black shales from the Wynniatt and Boot Inlet Formations D. van Acken, D. Thomson, R.H. Rainbird and R.A. Creaser	124
The Pan-African quartz-syenite of Guider (north-Cameroon): Magnetic fabric and U-Pb dating of a late-orogenic emplacement D. Dawai, J.-L. Bouchez, J.-L. Paquette and R. Tchameni	132
Tectonic evolution of the southeastern margin of the Yangtze Block: Constraints from SHRIMP U-Pb and LA-ICP-MS Hf isotopic studies of zircon from the eastern Jiangnan Orogenic Belt and implications for the tectonic interpretation of South China C. Yin, S. Lin, D.W. Davis, G. Xing, W.J. Davis, G. Cheng, W. Xiao and L. Li	145

(Contents continued on page 304)

CAPTION FOR COVER PHOTOGRAPH

3,243 million-year-old spherules in the Fig Tree Group, Barberton Greenstone Belt, South Africa, formed as a result of large meteorite impacts on the early Earth. The 35-cm-thick spherule bed (S3) is composed of nearly pure spherules produced during the condensation of an impact-produced rock vapor cloud. The estimated diameter of the bolide was 20–50 km. The spherules, 0.5–1.5 mm in diameter in the photo, include silica-(clear), phyllosilicate- (gray), and rutile/anatase-rich (black) varieties; massive and layered types; and a few originally hollow spherules. This is one of four spherule layers in the Barberton Belt, ranging from 3,470–3,243 Ma, that represent the oldest known impact deposits and provide direct evidence for a significant flux of large impactors as late as 3.2 Ga. Photograph: D.R. Lowe



(Contents continued from back cover)

Organic-walled microfossils from the early Neoproterozoic Liulaobei Formation in the Huainan region of North China and their biostratigraphic significance Q. Tang, K. Pang, S. Xiao, X. Yuan, Z. Ou and B. Wan	157
Geochemical, Sr-Nd isotopic, and zircon U-Pb geochronological constraints on the petrogenesis of Late Paleoproterozoic mafic dykes within the northern North China Craton, Shanxi Province, China S. Liu, C. Feng, B.-m. Jahn, R. Hu, S. Gao, G. Feng, S. Lai, Y. Yang, Y. Qi and I.M. Coulson	182
Overview of the magnetic signatures of the Palaeoproterozoic Rustenburg Layered Suite, Bushveld Complex, South Africa J. Cole, C.A. Finn and S.J. Webb	193
The Sugetbrak basalts from northwestern Tarim Block of northwest China: Geochronology, geochemistry and implications for Rodinia breakup and ice age in the Late Neoproterozoic B. Xu, H. Zou, Y. Chen, J. He and Y. Wang	214
A Rodinian suture in western India: New insights on India-Madagascar correlations C. Ishwar-Kumar, B.F. Windley, K. Horie, T. Kato, T. Hokada, T. Itaya, K. Yagi, C. Gouzu and K. Sajeev	227
The petrogenesis of calc-alkaline granites from the Elat massif, Northern Arabian-Nubian shield A. Weissman, R. Kessel, O. Navon and M. Stein	252
Geochronology and geochemistry of Neoproterozoic Mt. Abu granitoids, NW India: Regional correlation and implications for Rodinia paleogeography L.D. Ashwal, A.M. Solanki, M.K. Pandit, F. Corfu, B.W.H. Hendriks, K. Burke and T.H. Torsvik	265
Sedimentology, stratigraphy and geochemistry of a stromatolite biofacies in the 2.72 Ga Tumbiana Formation, Fortescue Group, Western Australia J.M. Coffey, D.T. Flannery, M.R. Walter and S.C. George	282
Reply to the discussion of Deb (2013) on the paper of Saha et al. (2013) entitled 'Tectono-magmatic evolution of the Mesoproterozoic Singhora basin, central India: Evidence for compressional tectonics from structural data, AMS study and geochemistry of basic rocks' P.P. Chakraborty, K. Das, S. Saha, P. Das, S. Karmakar and M.A. Mamtani	297
Corrigendum to "Seismic imaging of the Proterozoic Cuddapah basin, south India and regional geodynamics" [Precambrian Res. 231 (2013) 277-289] K. Chandrakala, D.M. Mall, D. Sarkar and O.P. Pandey	303

(Abstracts/contents lists published in Am. Geol. Inst. Bibliogr.; Abstr. Bull. Signalétique; Chem. Abstr.; Curr. Contents; Phys. Chem. Earth Sci., Geo Abstr.; Mineral Abstr.)

Depositional age of the early Paleoproterozoic Klipputs Member, Nelani Formation (Ghaap Group, Transvaal Supergroup, South Africa) and implications for low-level Re-Os geochronology and Paleoproterozoic global correlations B. Kendall, D. van Aken and R.A. Créaser	1
Paleoproterozoic metamorphic and deformation history of the Thompson Nickel Belt, Superior Boundary Zone, Canada, from in situ U-Pb analysis of monazite C.G. Couëslan, D.R.M. Pattison and S. Andrew Dufrane	13
Evidence for 2.0 Ga continental microbial mats in a paleodesert setting E.L. Simpson, E. Heness, A. Bumby, P.G. Eriksson, K.A. Eriksson, H.L. Hilbert-Wolf, S. Linnevelt, H.F. Malenda, T. Modungwa and O.J. Okafor	36
Constraints on the timing of the Tenaft Event and associated Au-Cu-Bi mineralisation in the Tennant Region, Northern Territory D.W. Maidment, D.L. Huston, N. Donnellan and A. Lambeck	51
Precambrian evolution of the Lhasa terrane, Tibet: Constraint from the zircon U-Pb geochronology of the gneisses Y.-H. Lin, Z.-M. Zhang, X. Dong, K. Shen and X. Lu	64
Geochronology and trace element geochemistry of zircon, monazite and garnet from the garnetite and/or associated other high-grade rocks: Implications for Palaeoproterozoic tectonothermal evolution of the Khondalite Belt, North China Craton S. Jiao, J. Guo, S.L. Harley and P. Peng	78
Eastward transport of the Monapo Klippe, Mozambique determined from field kinematics and computed tomography and implications for late tectonics in central Gondwana J.A. Miller, C. Faber, C.D. Rowe, P.H. Macey and A. du Plessis	101

CAPTION FOR COVER PHOTOGRAPH

3,243 million-year-old spherules in the Fig Tree Group, Barberton Greenstone Belt, South Africa, formed as a result of large meteorite impacts on the early Earth. The 35-cm-thick spherule bed (S3) is composed of nearly pure spherules produced during the condensation of an impact-produced rock vapor cloud. The estimated diameter of the bolide was 20–50 km. The spherules, 0.5–1.5 mm in diameter in the photo, include silica-(clear), phyllosilicate- (gray), and rutile/anatase-rich (black) varieties; massive and layered types; and a few originally hollow spherules. This is one of four spherule layers in the Barberton Belt, ranging from 3,470–3,243 Ma, that represent the oldest known impact deposits and provide direct evidence for a significant flux of large impactors as late as 3.2 Ga. Photograph: D.R. Lowe



(Abstracts/contents lists published in *Am. Geol. Inst. Bibliogr.*; *Abstr. Bull. Signalétique*; *Chem. Abstr.*; *Curr. Contents*; *Phys. Chem. Earth Sci.*; *Geo Abstr.*; *Mineral Abstr.*)

Geochronology and geochemistry of volcanic rocks from the Shaojiwa Formation and Xingzi Group, Lushan area, SE China: Implications for Neoproterozoic back-arc basin in the Yangtze Block L. Li, S. Lin, G. Xing, D.W. Davis, W.J. Davis, W. Xiao and C. Yin	1
Petrology of the high-Mg tonalites and dioritic enclaves of the ca. 2130 Ma Alto Maranhão suite: Evidence for a major juvenile crustal addition event during the Rhyacian orogenesis, Mineiro Belt, southeast Brazil L.A.R. Seixas, J.-M. Bardintzeff, R. Stevenson and B. Bonin	18
The sulfur isotope signatures of Marinoan deglaciation captured in Neoproterozoic shallow-to-deep cap carbonate from South China J. Huang, X. Chu, T.W. Lyons, T. Sun, L. Feng, Q. Zhang and H. Chang	42
Early differentiation of the bulk silicate Earth as recorded by the oldest mantle reservoir X.-C. Wang, Z.-X. Li and X.-H. Li	52
Metamorphic <i>P-T-t</i> paths retrieved from the amphibolites, Lushan terrane, Henan Province and reappraisal of the Paleoproterozoic tectonic evolution of the Trans-North China Orogen J.-S. Lu, G.-D. Wang, H. Wang, H.-X. Chen and C.-M. Wu	61
The Wernecke igneous clasts in Yukon, Canada: Fragments of the Paleoproterozoic volcanic arc terrane Bonnetia A.B. Nielsen, D.J. Thorkelson, H.D. Gibson and D.D. Marshall	78
Key paleomagnetic poles and their use in Proterozoic continent and supercontinent reconstructions: A review K.L. Buchan.....	93
Uranium and gold deposits in the Pine Creek Orogen (North Australian Craton): A link at 1.8 Ga? J. Mercadier, R.G. Skirrow and A.J. Cross	111
New age constraints for the Proterozoic Aravalli–Delhi successions of India and their implications N.R. McKenzie, N.C. Hughes, P.M. Myrow, D.M. Banerjee, M. Deb and N.J. Planavsky	120
Uranium-bearing hematite from the Olympic Dam Cu-U-Au deposit, South Australia: A geochemical tracer and reconnaissance Pb-Pb geochronometer C.L. Ciobanu, B.P. Wade, N.J. Cook, A. Schmidt Mumm and D. Giles	129
Diapirism and sagduction as a mechanism for deposition and burial of “Timiskaming-type” sedimentary sequences, Superior Province: Evidence from detrital zircon geochronology and implications for the Borden Lake conglomerate in the exposed middle to lower crust in the Kapuskasing uplift S. Lin, J. Parks, L.M. Heaman, A. Simonetti and M.T. Corkery	148
The Serra da Bolívia complex: The record of a new Neoproterozoic arc-related unit at Ribeira belt M. Heilbron, M. Tupinambá, C.d.M. Valeriano, R. Armstrong, L.G. do Eirado Siva, R.S. Melo, A. Simonetti, A.C. Pedrosa Soares and N. Machado	158
Revisiting the age and paleomagnetism of the Modipe Gabbro of South Africa S.W. Denyszyn, J.M. Feinberg, P.R. Renne and G.R. Scott	176

(Contents continued on BM I)

CAPTION FOR COVER PHOTOGRAPH

3,243 million-year-old spherules in the Fig Tree Group, Barberton Greenstone Belt, South Africa, formed as a result of large meteorite impacts on the early Earth. The 35-cm-thick spherule bed (S3) is composed of nearly pure spherules produced during the condensation of an impact-produced rock vapor cloud. The estimated diameter of the bolide was 20–50 km. The spherules, 0.5–1.5 mm in diameter in the photo, include silica-(clear), phyllosilicate- (gray), and rutile/anatase-rich (black) varieties; massive and layered types; and a few originally hollow spherules. This is one of four spherule layers in the Barberton Belt, ranging from 3,470–3,243 Ma, that represent the oldest known impact deposits and provide direct evidence for a significant flux of large impactors as late as 3.2 Ga. Photograph: D.R. Lowe



(Contents continued from back cover)

A Proterozoic boundary in southern Norway revealed by joint-inversion of P-receiver functions and surface waves M.L. Kolstrup and V. Maupin	186
Re-Os age constraints and new observations of Proterozoic glacial deposits in the Vazante Group, Brazil N.J. Geboy, A.J. Kaufman, R.J. Walker, A. Misi, T.F. de Oliviera, K.E. Miller, K. Azmy, B. Kendall and S.W. Poulton ...	199
Stratigraphy, palaeontology and geochemistry of the late Neoproterozoic Aar Member, southwest Namibia: Reflecting environmental controls on Ediacara fossil preservation during the terminal Proterozoic in African Gondwana M. Hall, A.J. Kaufman, P. Vickers-Rich, A. Ivantsov, P. Trusler, U. Linnemann, M. Hofmann, D. Elliott, H. Cui, M. Fedonkin, K.-H. Hoffmann, S.A. Wilson, G. Schneider and J. Smith	214



Contents

Special Issue JEBEL

Guest Editors:

Victoria Pease, Ghaleb H. Jarrar, Khalid Kadi, Mahmoud H. Shalaby

Preface

Introduction to the JEBEL volume of *Precambrian Research*

V. Pease and P.R. Johnson 1

Ediacaran sediments and igneous rocks

U-Pb detrital zircon provenance of the Saramuj Conglomerate, Jordan, and implications for the Neoproterozoic evolution of the Red Sea region

N. Yaseen, V. Pease, G.H. Jarrar and M. Whitehouse 6

Carbonatite crystallization and alteration in the Tarr carbonatite-albitite complex, Sinai Peninsula, Egypt

A. Boskabadi, I.K. Pitcairn, R.J. Stern, M.K. Azer, C. Broman, F.H. Mohamed and J. Majka 24

Cryogenian crustal growth, metamorphism, and climate

Hf isotopic composition of single zircons from Neoproterozoic arc volcanics and post-collision granites, Eastern Desert of Egypt: Implications for crustal growth and recycling in the Arabian-Nubian Shield

K.A. Ali, S.A. Wilde, R.J. Stern, A.M. Moghazi and S.M.M. Ameen 42

Geochemistry and *P-T-t* evolution of the Abu-Barqa Metamorphic Suite, SW Jordan, and implications for the tectonics of the northern Arabian-Nubian Shield

G.H. Jarrar, T. Theye, N. Yaseen, M. Whitehouse, V. Pease and C. Passchier 56

~750 Ma banded iron formation from the Arabian-Nubian Shield-Implications for understanding Neoproterozoic tectonics, volcanism, and climate change

R.J. Stern, S.K. Mukherjee, N.R. Miller, K. Ali and P.R. Johnson 79

Earlier framework

The Nabitah fault zone, Saudi Arabia: A Pan-African suture separating juvenile oceanic arcs

M.J. Flowerdew, M.J. Whitehouse and D.B. Stoeser 95

The Feiran-Solaf metamorphic complex, Sinai, Egypt: Geochronological and geochemical constraints on its evolution

M.M. Abu El-Enen and M.J. Whitehouse 106